Widths and asymmetries of the $K\alpha_1$ and $K\alpha_2$ x-ray lines and the L_2 and L_3 fluorescence yields of the transition elements

P. L. Lee and S. I. Salem
Department of Physics-Astronomy, California State University, Long Beach, California 90840
(Received 17 July 1974)

The $K\alpha_1$ and $K\alpha_2$ x-ray lines of the transition elements $23 \leq Z \leq 32$ were measured using an improved version of a single-crystal high-angle goniometer in conjunction with a NaI scintillation detector. The x-ray spectrum of these elements was produced by bombarding them with an electron beam of constant energy and flux. A computer program was devised and used to unfold the physical widths and the asymmetries of these lines. Previous experimental results on both linewidths and asymmetries are included for comparison. The interpretation of the asymmetries as the result of a simple exchange interaction is only partially satisfactory. Values of L_2 and L_3 fluorescence yields were extracted from the measured linewidths and compared with theory.

INTRODUCTION

The widths of the $K\alpha_1$ $[K\text{-}L_3]$ and the $K\alpha_2$ $[K\text{-}L_2]$ x-ray emission lines of the transition elements $21 \leq Z \leq 31$ were previously measured.[1-6] The results of most of these experiments were tabulated by Blokhin,[7] and the subject was reviewed by Parratt[8] and by Sevier.[9] The asymmetry of these lines has also been observed and measured,[10-12] and with some success has been explained as the result of the interaction between the $3d$ and the $2p$ electrons. Such an interaction splits each of the $2p_{3/2}$ and $2p_{1/2}$ electronic levels,[13] resulting in two and possibly more closely associated emission lines.

A similar condition exists in the rare-earth elements and results in the splitting of each of their $4p$ levels, and consequently splits the $L\beta_{2,15}$ $[L_3\text{-}N_{4,5}]$ and the $L\gamma_1$ $[L_2\text{-}N_4]$ x-ray lines.[14,15] This level splitting is still not well understood, but it is known to be basically atomic in nature, and any solid-state (chemical) effect that exists is relatively small.[15]

Theoretical calculations as well as experimental results[16] show that the widths of the $K\alpha_1$ and $K\alpha_2$ lines of elements with atomic number Z greater than 50 vary as $Z^{3.87}$, but a pronounced deviation from this trend occurs in the region $22 \leq Z \leq 35$, where the asymmetry of these lines add to their widths. Even if asymmetry contributions are removed, experimental linewidths are significantly larger than their theoretically expected value.

The observed frequency distribution $f(\nu')$ of x-ray photons within an x-ray emission line may be written as

$$f(\nu') = \int_{-\infty}^{\infty} \psi(\nu')\phi(\nu - \nu')\,d\nu', \qquad (1)$$

where ψ is the physical distribution, ϕ is the instrumental response, ν' is the frequency of radiation, and ν is the frequency at the center of the peak. Equation (1) can be solved only if the functions ψ and ϕ are explicitly known. Several attempts at determining the shape of the physical distribution and instrumental response were made; the most successful in fitting experimental data assumes that the lineshape is Lorentzian and the instrumental response is Gaussian.[16]

In previous studies of the widths and asymmetries of the $K\alpha_1$ and $K\alpha_2$ emission lines of the transition elements, the experimental data were manually analyzed. In this work, the natural widths and the asymmetries of these lines were unfolded using a computer program.

The L_2 and L_3 fluorescence yields have never been measured in this region of low atomic number. Making use of the measured values of the $K\alpha_1$ and $K\alpha_2$ x-ray linewidths, Scofield's theoretical values of radiative widths,[17] and the values of nonradiative widths from Kostroun *et al.*,[18] the fluorescence yields of the L_2 and L_3 subshells were calculated and compared with the results of the most recent theoretical calculations.

EXPERIMENTAL

The $K\alpha_1$ and $K\alpha_2$ x-ray emission lines of ten elements, $23 \leq Z \leq 32$, were studied. Except for $_{31}$Ga and $_{32}$Ge the elements were blocks 99.9% pure, which were tightly fitted to a water-cooled anode assembly prior to introducing them into the vacuum chamber. Both $_{31}$Ga and $_{32}$Ge samples were placed in a $_{29}$Cu dish, which in turn was fitted to the anode assembly. These elements were ionized by an electron beam of constant energy and flux, which was provided by a $_{74}$W filament fitted in a stainless-steel focusing cup. An insulated transformer supplied the filament with

the heating current. A power supply connected in series with a voltage regulator and a ripple suppressor and rated at less than 0.3% ripple at a full load of 120 keV and 30 mA was used to accelerate the electron beam. The studied samples were exposed to the electron beam in a locally designed and built x-ray tube which was continuously pumped to a pressure of about 10^{-6} mm of Hg. Generally the samples were bombarded with an electron beam of 0.5 mA and 30 keV. These two quantities were constant to within 5% for the duration of the run.

The $K\alpha_1$ and $K\alpha_2$ lines of these elements were analyzed using a modified single-crystal high-angle goniometer and a NaI scintillation detector. This was performed by stepping the spectrometer through the Bragg angle 2θ in steps of 0.005°. At each position the intensity was measured by counting the photons emitted during a 1-min interval. At least three runs were measured for each element. A sample spectrum is shown in Fig. 1.

The unfolding of the asymmetry and linewidth of the $K\alpha_1$ and $K\alpha_2$ emission lines was performed by a least-squares–fitting program using a CDC 3150 computer. The shape of each of these lines was represented by two Lorentzians, whose peak centers are separated by a quantity δ and whose relative heights are H_a and H_b, in the following fashion:

$$\psi(\nu') = \frac{H_a}{(\nu'-\nu)^2+(\tfrac{1}{2}\Gamma)^2} + \frac{H_b}{(\nu'-\nu-\delta)^2+(\tfrac{1}{2}\Gamma)^2} . \quad (2)$$

Knowing that δ is small compared to Γ, one is justified in expanding the second term in Eq. (2) and retaining only the first-order term in δ. Thus Eq. (2) reduces to

$$\psi(\nu') = \frac{H}{(\nu'-\nu)^2+(\tfrac{1}{2}\Gamma)^2}\left(1+\frac{\nu'-\nu}{(\nu'-\nu)^2+(\tfrac{1}{2}\Gamma)^2}\,\frac{\Gamma}{2}\,\beta\right), \quad (3)$$

where the parameters H_a, H_b, and δ that appear in Eq. (2) are combined to give the new parameters H and β. The asymmetry index α is given in terms of the parameter β by the relation

$$\alpha = (2-\beta^2+\beta)/(2-\beta^2-\beta), \quad (4)$$

and α is defined as the ratio of the distances measured at half-maximum from the position of maximum intensity to the line contours at the long-wavelength and short-wavelength sides.

The instrumental response ϕ is assumed to be Gaussian in shape. Thus the experimental line contour is fitted by a 10-parameter expression:

$$f(\nu_i) = P_1 + P_2\nu_i + P_3\int_{-\infty}^{\infty}\int_{\nu_i-s/2}^{\nu_i+s/2}\frac{\exp[-4\ln 2(\xi/\sigma_1)^2]}{(\nu_i'-P_4+\xi)^2+(\tfrac{1}{2}P_9)^2}\left(1+\frac{\nu_i'+P_4+\xi}{(\nu_i'+P_4+\xi)^2+(\tfrac{1}{2}P_7)^2}\,\frac{P_7}{2}\,P_9\right)d\nu'\,d\xi$$

$$+P_5\int_{-\infty}^{\infty}\int_{\nu_i-s/2}^{\nu_i+s/2}\frac{\exp[-4\ln 2(\xi/\sigma_2)^2]}{(\nu_i'-P_6+\xi)^2+(\tfrac{1}{2}P_8)^2}\left(1+\frac{\nu'+P_6+\xi}{(\nu_i'+P_6+\xi)^2+(\tfrac{1}{2}P_8)^2}\,\frac{P_8}{2}\,P_{10}\right)d\nu'\,d\xi, \quad (5)$$

where P_1 is the background, P_2 is its slope, and P_3 and P_5 are the peak heights of the $K\alpha_1$ and $K\alpha_2$, respectively. The position of the peak centers of these lines are given by P_4 and P_6 and their widths by P_7 and P_8, while P_9 and P_{10} are the values of the parameter β defined in Eq. (3) for the $K\alpha_1$ and $K\alpha_2$ lines, respectively, and s is the slit width.

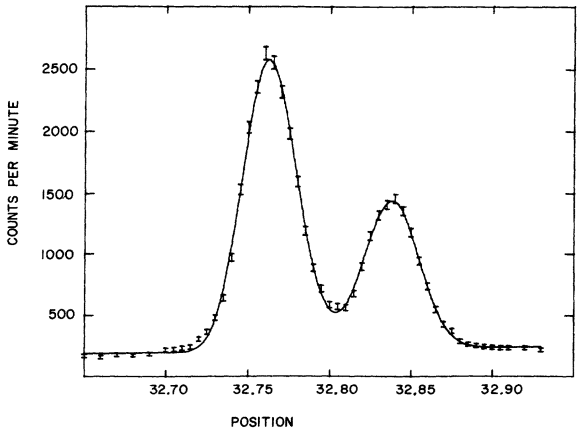

FIG. 1. $K\alpha_1$ and $K\alpha_2$ lines of $_{28}$Ni. The error bars represent statistical errors and the smooth curve is from Eq. (5).

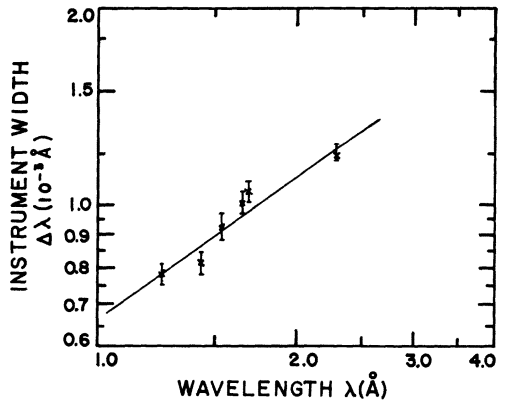

FIG. 2. Instrumental width as a function of the wavelength.

TABLE I. Linewidth and asymmetry of the $K\alpha_1$ and $K\alpha_2$ lines of the transition elements.

Elements	$K\alpha_1$ Linewidth $\Gamma_{K\alpha_1}$ (eV)	$K\alpha_1$ Asymmetry	$K\alpha_2$ Linewidth $\Gamma_{K\alpha_2}$ (eV)	$K\alpha_2$ Asymmetry
$_{23}$V	1.80 ± 0.17	1.17 ± 0.12	2.25 ± 0.22	1.12 ± 0.11
$_{24}$Cr	2.16 ± 0.22	1.38 ± 0.13	2.75 ± 0.30	1.18 ± 0.12
$_{25}$Mn	2.13 ± 0.19	1.35 ± 0.14	2.60 ± 0.25	1.26 ± 0.13
$_{26}$Fe	2.35 ± 0.21	1.43 ± 0.14	2.84 ± 0.26	1.25 ± 0.13
$_{27}$Co	2.87 ± 0.29	1.32 ± 0.13	3.59 ± 0.37	1.25 ± 0.13
$_{28}$Ni	2.89 ± 0.27	1.19 ± 0.12	3.64 ± 0.35	1.20 ± 0.12
$_{29}$Cu	2.56 ± 0.19	1.12 ± 0.11	4.05 ± 0.33	1.10 ± 0.11
$_{30}$Zn	2.86 ± 0.26	1.09 ± 0.11	3.99 ± 0.36	1.12 ± 0.11
$_{31}$Ga	3.04 ± 0.31	1.00 ± 0.10	4.10 ± 0.41	1.00 ± 0.10
$_{32}$Ge	3.74 ± 0.31	1.04 ± 0.10	4.41 ± 0.40	1.05 ± 0.10

The half-widths of the instrumental response functions for the $K\alpha_1$ and the $K\alpha_2$ are σ_1 and σ_2, respectively. To determine the unknown parameters σ_1 and σ_2, Eq. (5) was fitted to the experimental line contour using values for P_7 and P_8 from Ref. 7. The values of σ_1 and σ_2 thus obtained were put back in Eq. (5) and a second least-squares fit provided new values for P_7 and P_8. After two or three iterations, a constant set of values for P_7, P_8, σ_1, and σ_2 was obtained. The values of the half-widths of the instrumental response σ are plotted as a function of the wavelength in Fig. 2. The straight line joining the experimental points corresponds to the most probable values. (This is the same instrumental response used to determine the linewidths of the L spectrum of the rare-earth elements in the following paper.)

Equation (5), with known values of σ_1 and σ_2, was fitted to the experimental line contours to determine the linewidth and asymmetry.

RESULTS AND DISCUSSION

The measured $K\alpha_1$ and $K\alpha_2$ linewidths and asymmetries are shown in Table I and are also plotted

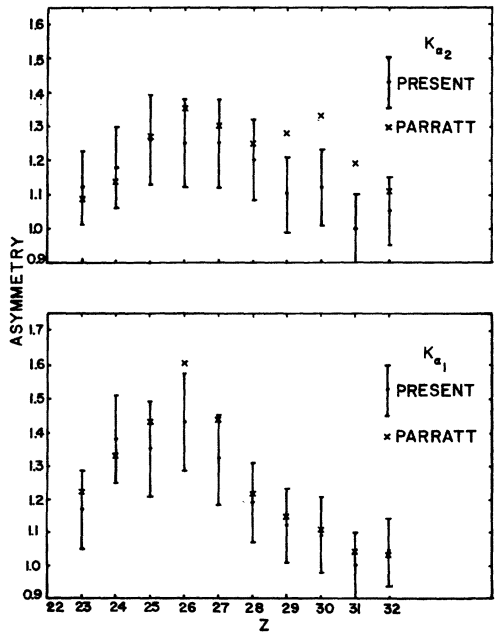

FIG. 3. Asymmetry index α of the $K\alpha_1$ and $K\alpha_2$ lines plotted as functions of atomic number.

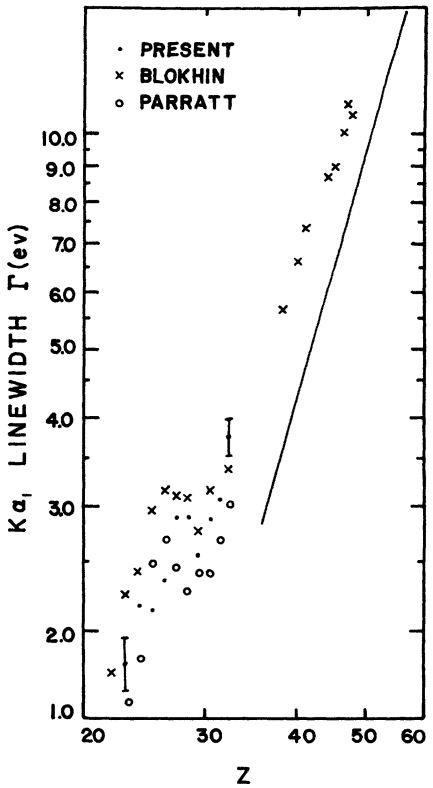

FIG. 4. $K\alpha_1$ linewidth plotted as a function of atomic number. The straight line exhibits the $Z^{3.87}$ dependence.

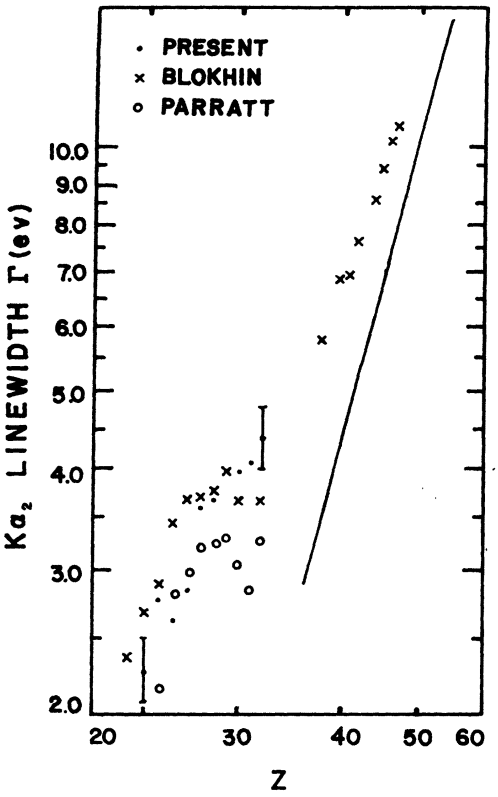

FIG. 5. $K\alpha_2$ linewidth plotted as a function of atomic number. The straight line exhibits the $Z^{3.87}$ dependence.

as functions of atomic numbers in Figs. 3–5. Also shown in these diagrams are the results of some previous experiments. Our values of linewidths agree within experimental errors with the previously reported values for both $K\alpha_1$ and $K\alpha_2$ lines. Although the present values of asymmetry and

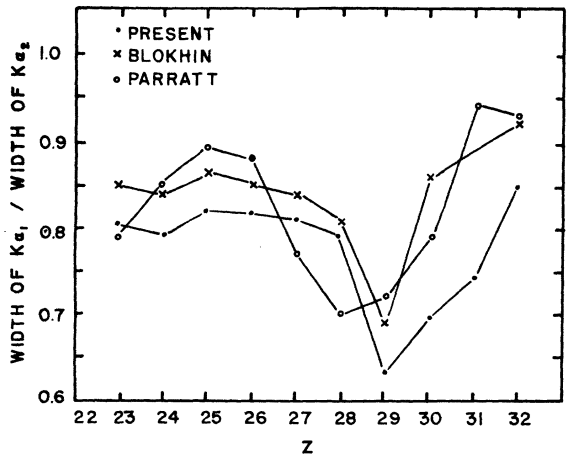

FIG. 6. Ratio of the $K\alpha_2$ linewidth to the $K\alpha_1$ linewidth plotted as a function of atomic number.

those of Parratt agree rather well in the case of the $K\alpha_1$ line, Parratt's values are higher than the present results for the $K\alpha_2$ line, especially for the higher-Z elements.

The errors quoted in Table I and shown in Figs. 2–5 for linewidths and line asymmetries are statistical errors obtained from the error matrix of the least-squares-fit program.

Of interest is the ratio of the linewidth of the $K\alpha_1$ line to that of the $K\alpha_2$ line shown in Fig. 6. The pronounced dip at $_{29}$Cu and the smaller one at $_{24}$Cr are of significance as both elements have only one electron in the $4s$ state.

Several workers have proposed various explanations to this observed asymmetry or line splitting. Tsutsumi[19] showed that the line splitting could not be due to multiple ionizations and elaborated on a splitting caused by the Coulomb exchange interaction between the hole in the $2p$ level and the

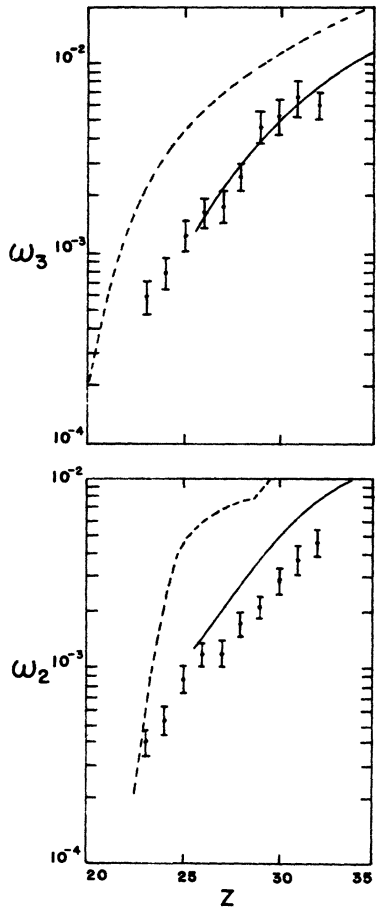

FIG. 7. Fluorescence yield ω_2 of the L_2 subshell and ω_3 of the L_3 subshell plotted as functions of atomic number. The points are obtained from experimental linewidths, Eqs. (6) and (7). The solid curves are from Ref. 23 and the dashed curves are from Ref. 22.

TABLE II. Fluorescence yield of the L_2 and L_3 shells calculated from the experimental values of the $K\alpha_1$ and $K\alpha_2$ x-ray linewidths.

Elements	Γ^K_{rad} (eV) (Ref. 17)	Γ^K_{nonrad} (eV) (Ref. 18)	$\Gamma^{L_2}_{rad}$ (eV) (Ref. 17)	L_2 fluorescence yield ($\omega_2 \times 10^3$)	$\Gamma^{L_3}_{rad}$ (eV) (Ref. 17)	L_3 fluorescence yield ($\omega_3 \times 10^3$)
$_{23}$V	0.228	0.710	5.21(−4)	0.40 ± 0.07	5.19(−4)	0.60 ± 0.12
$_{24}$Cr	0.276	0.725	9.24(−4)	0.53 ± 0.09	9.17(−4)	0.79 ± 0.15
$_{25}$Mn	0.333	0.740	1.34(−3)	0.88 ± 0.14	1.33(−3)	1.26 ± 0.23
$_{26}$Fe	0.396	0.754	1.99(−3)	1.18 ± 0.18	1.97(−3)	1.64 ± 0.29
$_{27}$Co	0.469	0.768	2.86(−3)	1.21 ± 0.19	2.82(−3)	1.73 ± 0.31
$_{28}$Ni	0.551	0.780	3.97(−3)	1.72 ± 0.27	3.91(−3)	2.51 ± 0.44
$_{29}$Cu	0.643	0.791	5.50(−3)	2.10 ± 0.27	5.39(−3)	4.78 ± 0.83
$_{30}$Zn	0.747	0.802	7.15(−3)	2.93 ± 0.49	7.01(−3)	5.35 ± 1.10
$_{31}$Ga	0.864	0.818	9.12(−3)	3.77 ± 0.68	8.94(−3)	6.58 ± 1.50
$_{32}$Ge	0.996	0.833	11.4(−3)	4.52 ± 0.72	11.2(−3)	6.03 ± 1.00

electrons in the partially filled $3d$ shell. Although his calculations seem to agree with observed values for elements with nearly half-filled $3d$ shells (Mn, Fe, and Co), the agreement is poor for both higher- and lower-Z elements. Nefedov[20] introduced spin-orbit coupling with some success while Ekstig *et al.*[21] performed a more detailed analysis and considered the entire transition sequence, but their results gave only qualitative agreement. It is quite logical to conclude that the asymmetry of these lines is at least partially caused by the $2p$-$3d$ exchange interaction, but it is more than likely that some other effects are also present.

FLUORESCENCE YIELD

The fluorescence yield ω_2 of the L_2 subshell may be calculated from the linewidth $\Gamma_{K\alpha_2}$ of the $K\alpha_2$ line, the radiative widths Γ^K_{rad} and $\Gamma^{L_2}_{rad}$ of the K shell and L_2 subshell, respectively, and the nonradiative width Γ^K_{nonrad} of the K shell:

$$\omega_2 = \Gamma^{L_2}_{rad} / (\Gamma_{K\alpha_2} - \Gamma^K_{rad} - \Gamma^K_{nonrad}) . \quad (6)$$

Similarly, the fluorescence yield ω_3 of the L_3 subshell may be written as

$$\omega_3 = \Gamma^{L_3}_{rad} / (\Gamma_{K\alpha_1} - \Gamma^K_{rad} - \Gamma^K_{nonrad}) . \quad (7)$$

Values of the fluorescence yields ω_2 and ω_3 were thus calculated using the experimental values of the linewidths from Table I, theoretical values of the radiative widths from Scofield's theory,[17] and the values of the nonradiative widths from Kostroun *et al.*[18] These results are presented in Table II and are plotted in Fig. 7. Also plotted are the theoretical values of the fluorescence yields of McGuire[22] and Chen *et al.*[23] The theoretical values of McGuire are considerably higher for both ω_2 and ω_3. The present values calculated for ω_3 are in excellent agreement with the theoretical values of Chen *et al.*, but the present values of ω_2 are slightly lower than the theoretical values.

The reported errors for both ω_2 and ω_3 are the results of the errors reported for the $K\alpha_1$ and $K\alpha_2$ linewidths only; i.e., in determining the fluorescence-yield errors, no uncertainty was assigned to the theoretical values of the radiative and nonradiative widths.

[1] L. G. Parratt, Phys. Rev. 44, 695 (1933).
[2] S. K. Allison, Phys. Rev. 44, 63 (1933).
[3] S. K. Allison and J. H. Williams, Phys. Rev. 35, 1476 (1930).
[4] F. K. Richtmyer and S. W. Barnes, Phys. Rev. 46, 252 (1934).
[5] H. H. Roseberry and J. A. Bearden, Phys. Rev. 50, 204 (1936).
[6] L. G. Parratt, Phys. Rev. 50, 1 (1936).
[7] M. A. Blokhin, *The Physics of X-Rays*, 2nd edition (State Pub. House of Tech.-Theor. Lit., Moscow, 1957), p. 404 (English translation by U. S. AEC Office of Technical Inf.).
[8] L. G. Parratt, Rev. Mod. Phys. 31, 616 (1959).
[9] K. D. Sevier, *Low Energy Electron Spectroscopy* (Wiley, New York, 1972), p. 220.
[10] L. G. Parratt, Phys. Rev. 50, 1 (1936).
[11] J. A. Bearden and C. H. Shaw, Phys. Rev. 48, 18 (1935).
[12] T. Snyder, Phys. Rev. 59, 689 (1941).
[13] E. E. Wainstein, C. R. (Dokl.) Acad. Sci. URSS 40, 102 (1943).
[14] S. I. Salem, C. W. Schultz, B. A. Rabbani, and R. T. Tsutsui, Phys. Rev. Lett. 27, 477 (1971).

[15]S. I. Salem and Bruce L. Scott, Phys. Rev. A 9, 690 (1974).
[16]G. C. Nelson, W. John, and B. G. Saunders, Phys. Rev. 187, 1 (1969); Phys. Rev. A 2, 542 (1970).
[17]J. H. Scofield, Phys. Rev. 179, 9 (1969); and UCRL Report No. UCRL-51231, 1972 (unpublished).
[18]V. O. Kostroun, M. H. Chen, and B. Crasemann, Phys. Rev. A 3, 533 (1971).
[19]K. Tsutsumi, J. Phys. Soc. Japan 14, 1696 (1959); K. Tsutsumi and H. Nakamori, J. Phys. Soc. Japan 25, 1418 (1968).
[20]V. I. Nefedov, J. Struct. Chem. 5, 603 (1964); 7, 672 (1966).
[21]B. Ekstig, E. Källne, E. Norland, and R. Manne, Phys. Scr. 2, 38 (1970).
[22]E. J. McGuire, Phys. Rev. A 3, 587 (1971).
[23]M. H. Chen, B. Crasemann, and V. O. Kostroun, Phys. Rev. A 4, 1 (1971).